



**Calhoun: The NPS Institutional Archive**  
**DSpace Repository**

---

Faculty and Researchers

Faculty and Researchers' Publications

---

2009

## Tunable NIR Quantum Well Infrared Photodetector Using Interband Transitions

Alves, Fabio D.P.; Santos, Ricardo A.T.; Nohra, Luis F.M.;  
Magalhães, Luciano B.; Karunasiri, Gamani

IEEE

---

Alves, Fabio DP, et al. "Tunable NIR quantum well infrared photodetector using interband transitions." Microwave and Optoelectronics Conference (IMOC), 2009 SBMO/IEEE MTT-S International. IEEE, 2009.

<http://hdl.handle.net/10945/60326>

---

This publication is a work of the U.S. Government as defined in Title 17, United States Code, Section 101. Copyright protection is not available for this work in the United States.

*Downloaded from NPS Archive: Calhoun*



Calhoun is the Naval Postgraduate School's public access digital repository for research materials and institutional publications created by the NPS community. Calhoun is named for Professor of Mathematics Guy K. Calhoun, NPS's first appointed -- and published -- scholarly author.

**Dudley Knox Library / Naval Postgraduate School**  
**411 Dyer Road / 1 University Circle**  
**Monterey, California USA 93943**

<http://www.nps.edu/library>

# Tunable NIR Quantum Well Infrared Photodetector Using Interband Transitions

Fabio D. P. Alves, Ricardo A. T. Santos, Luis F. M.  
Nohra and Luciano B. Magalhães  
Instituto Tecnológico de Aeronáutica  
São José dos Campos, SP, Brazil  
durante@ita.br

Gamani Karunasiri  
Naval Postgraduate School  
Monterey, CA, USA  
gkarunas@nps.edu

**Abstract**— This paper presents the design and characterization of a near infrared (NIR) tunable quantum well infrared photodetector (QWIP). The detection was achieved using interband electron transitions between quantized energy levels for holes (light and heavy) in the valence band and quantized energy levels for electrons in the conduction band. The quantum wells are made asymmetric (step wells) to allow transitions between energy levels with different parity quantum numbers. The structure is modeled by solving self-consistently the Schrödinger and Poisson equations with the help of the shooting method. The photocurrent of the fabricated GaAs/InGaAs photodetector is measured at the temperature of 10 K and the observed response lies between 825 and 940 nm. When the bias is 0.5 V, a narrow response centered in 840 nm is achieved. Applying 4.5 V the peak response moves to 930 nm. The results demonstrate the possibility of tunable detection in the NIR band with great versatility.

**Keywords**— quantum-well; interband transition; photodetection; near-infrared

## I. INTRODUCTION

When one thin semiconductor layer (well) is sandwiched between two layers of larger bandgap material (barriers), a quantum well is formed. The potential profile is defined basically by the band offsets, allowing the existence of the quantized energy levels, confined inside the wells. Such structures allow the exploration of quantum effects that have become very useful in optoelectronic devices [1], particularly, when it is possible to detect photon absorption in quantum well infrared photodetectors (QWIPs) [2].

QWIPs are basically periodic repetitions of the *barrier/well/barrier* structure between heavy doped contact layers grown epitaxially on a semi-insulating substrate. When such structures are exposed to an incident photon flux, transitions between quantized energy levels can occur. The photon flux can be sensed when bias is applied to the contact layers and the transitions allow the extraction of the electrons from the well to the barrier regions, leading to a photocurrent. When the final state is confined, the electrons must tunnel through the potential barriers, made thinner by the applied electric field. Once the electron has escaped the confinement of the well, it accelerates toward the positive contact until it is captured.

Transitions between different states in quantum wells can occur in many ways. Nonetheless, two types of transitions, caused by a time-varying electromagnetic perturbation (incident photon flux), are of special interest: intersubband transitions, in which an electron moves from one subband to another, while remaining in the same band (conduction or valence), are more likely to be found in mid-wavelength infrared (MWIR) and long-wavelength infrared (LWIR) QWIPs [2]; and interband transitions, in which an electron in a valence subband can be excited to a conduction subband, can be found in optical modulators [3] and multiband detectors [4].

In the realm of QWIPs a great effort was made in the past 20 years to make these devices commercially available for a variety of applications. High sensitivity, high selectivity, and multispectral detection are the most attractive characteristics of these detectors. The advances in material sciences and semiconductor growth technology have allowed the use of bandgap engineering to cover, ideally, all IR bands [2]. Although NIR detection devices are traditionally bulk detectors due to the higher quantum efficiency [5], QWIPs can provide narrow band response and the peaks can be tuned according to the IR signature to be detected.

In this context it is reported in this paper a NIR QWIP with the spectral response adjustable by the applied bias using interband transitions.

## II. QWIP DESIGN

### A. Theoretical Aspects

The shortest wavelength detected using intersubband transitions reported in the literature [5] is about 2.7  $\mu\text{m}$ . In Addition, bulk detection is limited by the bandgap of the semiconductor. Thus, interband transitions are more appropriate to achieve detection of wavelengths higher than the obtained in bulk transitions and lower than the achieved using intersubband transitions.

In the general sense, the transition rate from an initial state represented by  $\Psi_{ik_i}$  to final states represented by  $\Psi_{fk_f}$ , due to an interaction potential,  $V_p$ , can be calculated using Fermi's golden rule [1]:

$$W(\Psi_{ik_i} \rightarrow \Psi_{fk_f}) = \frac{2\pi}{\hbar} \left| \langle \Psi_{fk_f} | V_p | \Psi_{ik_i} \rangle \right|^2 \delta(E_{ik_i} - E_{fk_f} - \hbar\omega). \quad (1)$$

In equation (1),  $\hbar\omega$  is the incident photon energy, and the delta function accounts for conservation of energy. The term in the Dirac notation is called electric dipole matrix element. The wavefunctions  $\Psi_n$  can be expressed by a combination of the envelope function  $\psi_n(r)$  and the cell periodic functions near the band extreme  $u_n(r)$  [1], written as:

$$\Psi_n = \psi_n(z)A^{-\frac{1}{2}}e^{ik_{xy}\rho}u_n(r), \quad (2)$$

where  $A$  is the in-plane normalization area,  $k_{xy}$  is the 2D wavevector ( $k_x, k_y$ ) and  $\rho$  represents the 2D in-plane vector. The matrix element in Equation (1) becomes:

$$\begin{aligned} \langle \Psi_{fk_f} | V_p | \Psi_{ik_i} \rangle = \\ \frac{1}{A} \langle \psi_{fk_f}(z) u_{fk_f}(r) e^{ik_{xy}\rho} | V_p | \psi_{ik_i}(z) u_{ik_i}(r) e^{ik_{xy}\rho} \rangle. \end{aligned} \quad (3)$$

Considering the fact that the envelope functions (related to the band-offset/electrostatic potential) vary slowly in the  $z$  direction compared to the cell periodic functions (related to the lattice potential), and for the optical transitions the initial and final states should have the same momentum ( $k_f = k_i$ ), the matrix element can be approximated by [6].

$$\langle \Psi_f | V_p | \Psi_i \rangle = \frac{1}{A} \left( \langle u_f(r) | V_p | u_i(r) \rangle \langle \psi_f(z) | \psi_i(z) \rangle + \langle \psi_f(z) | V_p | \psi_i(z) \rangle \langle u_f(r) | u_i(r) \rangle \right) \quad (4)$$

For the transitions between valence and conduction subbands, given that  $k_i$  and  $k_f$  are the same and are far from the edge of the Brillouin zone (otherwise the envelope function approximation is not valid), the cell periodic functions are orthogonal. This cancels out the second term in the right hand side of (4). Thus, combining (1) and (4) it is possible to notice that the rate of transition is proportional to the absolute value squared of the overlap of the envelope functions of the initial and final states,  $|\langle \Psi_f | V_p | \Psi_i \rangle|^2$ . Due to the orthogonality of the envelope functions in symmetric wells, transitions between subbands with different quantum numbers are forbidden. To allow these transitions the symmetry of the quantum well must be broken and it is commonly done using step wells.

### B. QWIP Configuration

The NIR detection is achieved using an undoped asymmetric step quantum well where electrons transitions, from heavy and light hole states (HH $n$  and LH $n$ , respectively) and electron confined states ( $n$ ), caused by an incident photon flux, can be converted in electric current. Fig. 1 shows the band diagram of the structure.

The structure is designed to have at least two confined subbands of each carrier in each band. In Fig. 1, the most probable transitions are HH1 $\rightarrow$ 1, HH2 $\rightarrow$ 2, LH1 $\rightarrow$ 1 and LH2 $\rightarrow$ 2. Although transitions between different parity quantum numbers are possible due to the asymmetry, they are less probable.

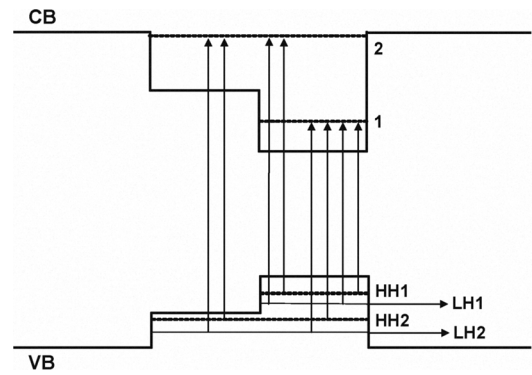


Figure 1. Asymmetric step quantum well band diagram with possible interband transitions (arrows). The acronyms HH $n$ , LH $n$  and  $n$  stand for heavy hole, light hole and electron confined states.

When bias is applied to the structure the potential profile bends making the barrier thinner and, consequently, increasing the tunneling probability. The electrons from the transition HH2 $\rightarrow$ 2 easily tunnel through the tip of the barrier, being the main contribution to the current. When the applied bias is increased, the excited state in the conduction band is pushed to the continuum due to the stark effect. When this happens, the oscillator strength of this transition is drastically reduced. In addition, the barrier is made even thinner, allowing the electrons from the transition HH1 $\rightarrow$ 1 to tunnel through and become the predominant contribution to the current. Intermediate bias levels can balance both contributions with the other transitions and give a more flat response all over the sensitivity range.

A configuration based on several repetitions of GaAs/InGaAs cells, growth on GaAs substrate were selected for this detector due to the reliability of material data (properties) found in the literature, lower cost and maturity of crystal growth processes and device fabrication. The barriers are made large enough to uncouple the wells. Contact layers are placed before and after the structure to allow the application of bias and current readout.

### C. Structure Description

To be able to design such structure it is necessary to build the potential profile based on the semiconductor properties and obtain the quantized energy levels inside the quantum wells as well as their respective wavefunctions. The electron wavefunctions in the structure were obtained using the effective mass approximation for the one-dimensional potential profile along the growth direction. For the valence band, the heavy and light hole bands were represented using average negative effective masses,  $m_{hh}$  and  $m_{lh}$ , respectively. In this case, the well potential is a confining potential for holes and the same model used for electrons in the conduction band is applicable. The Schrödinger's equations are numerically solved using the shooting method due to its ability to handle arbitrary potential profiles making the design more flexible [7].

This research was sponsored in part by Brazilian Air Force.

Several trials were executed varying the dimensions and the compositions of each layer resulting in a multilayered device shown schematically in Fig 2.

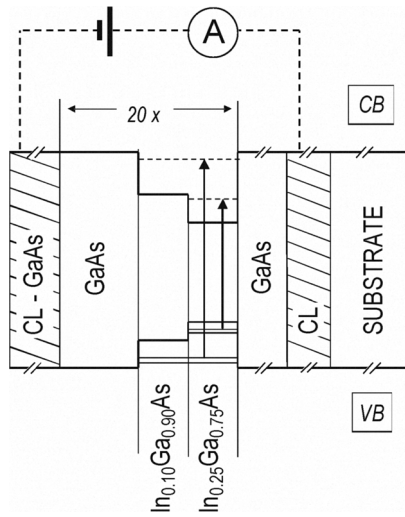


Figure 2. Schematic band diagram of NIR QWIP with the main transitions (arrows). CL stands for contact layer. The layers are off-scale. The dashed line represents the connections of the bias source and the A-meter to the device.

The fabricated photodetector consists of 600x200  $\mu\text{m}$  mesas with 64 semiconductor layers grown by molecular beam epitaxy (MBE) on a GaAs substrate as follows: a  $2 \times 10^{18} \text{ cm}^{-3}$  Si doped GaAs (0.7  $\mu\text{m}$ ) buffer layer, followed by 20 periods of undoped GaAs (300  $\text{\AA}$ )/In<sub>0.10</sub>Ga<sub>0.90</sub>As (43  $\text{\AA}$ )/In<sub>0.25</sub>Ga<sub>0.75</sub>As (40  $\text{\AA}$ )/GaAs (300  $\text{\AA}$ ) step quantum wells, ended by a  $2 \times 10^{18} \text{ cm}^{-3}$  Si doped GaAs (0.5  $\mu\text{m}$ ) contact layer.

### III. EXPERIMENTAL RESULTS

#### A. $I$ - $V$ Characteristics

The  $I$ - $V$  characteristics in dark were measured using an Agilent 4155B semiconductor parameter analyzer with the device inside a cold head where the temperature could be controlled. The first set of measurements was performed with the device surrounded by a cold aluminum foil to shield the background infrared radiation. The second set was performed removing the shield to determine the influence of the background radiation.

The measured  $I$ - $V$  characteristics for the NIR quantum well device as a function of temperature with the cold aluminum shield in place is shown in Fig 3.

The relatively large energy difference between the initial and final states limits thermally assisted tunneling and, the absence of free carriers (no doping) in the conduction band limits the thermionic emission, keeping the dark current below  $10^{-10} \text{ A}$  up to almost 4 V of applied bias. The clutter seen at low bias is most likely caused by the noise imposed by limitations of the analyzer.

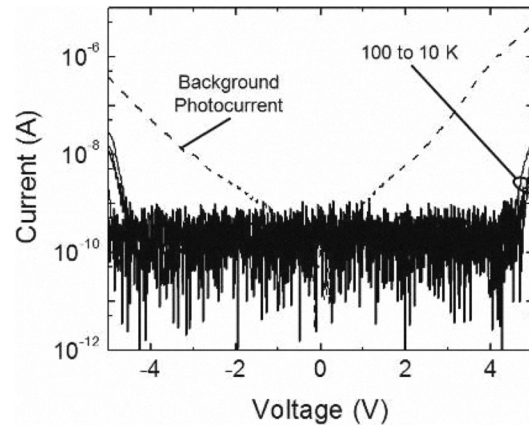


Figure 3.  $I$ - $V$  characteristics of NIR detector with cold aluminum shield for temperatures from 10 to 100 K with 10 K steps. The dashed curve corresponds to  $I$ - $V$  without the shield at 10 K.

At high bias ( $> 4.0\text{V}$ ), the background current raises more drastically due to field assisted tunneling of electrons through the barrier formed between the doped contacts and the undoped multiple quantum well structure. In addition, for those voltages, the curves for different temperatures follow almost the same path indicating that for these quantum wells, the temperature dependence of the dark current is very small.

#### B. Responsivity

##### 1) Experimental Setup

To permit the estimation of the device responsivity the photocurrent was measured between 800 and 960 nm. Fig. 4 shows the schematic diagram of the experimental setup and the estimation sequence.

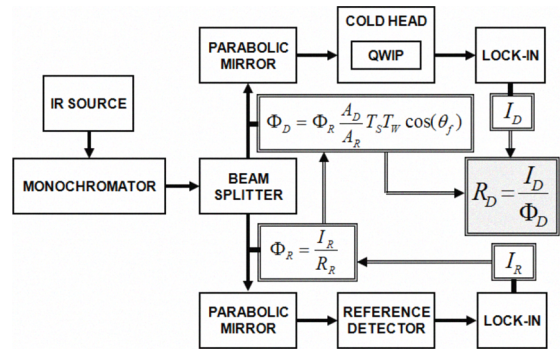


Figure 4. Schematic diagram of the experimental setup used to perform the photocurrent spectroscopy of the NIR QWIP.

The  $IR$  radiation passes through a monochromator, it is modulated by a chopper and divided equally in two beams. The first beam passes through a reference detector, with known responsivity, and its photocurrent is measured by a lock-in amplifier. This procedure allows to calculate the electron flux at the detector ( $\Phi_R$ ) and estimate the electron flux going into the test detector ( $\Phi_D$ ), considering the detectors area ratio

$(A_D/A_R)$ , transmission coefficient of the cold head window ( $T_W$ ), transmission coefficient of the substrate ( $T_S$ ) and the angle of the coupling face ( $\cos(\theta)$ ).

The second beam goes to the QWIP sample device placed into a cold head and connected as shown in Fig. 2. The light couples normal to the 45 degree face. The QWIP photocurrent is measured by another lock-in amplifier and the responsivity estimated as shown by the equation sequence in Fig. 4. In order to remove the background variation effects, measurements were carried with the source shutter closed before and after each scan. The average level of background was subtracted from the overall signal.

## 2) Results

Fig. 5 shows the absolute responsivity curves at 10 K for bias of 0.5 and 4.5 V. In the figure, the theoretical interband transition wavelengths are indicated by the arrows.

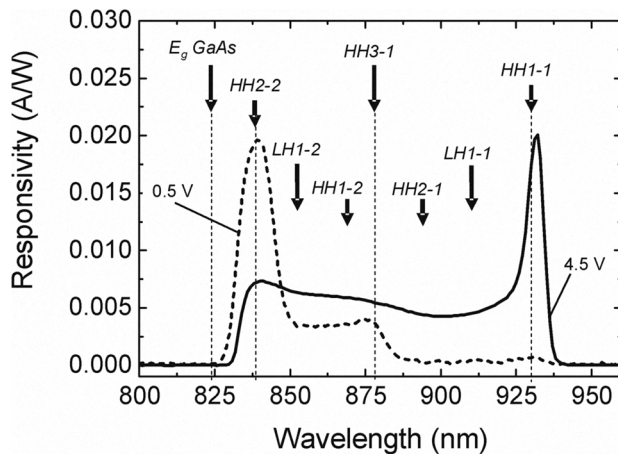


Figure 5. Responsivity of the NIR quantum well at 10 K, for 0.5 and 4.5 V of forward bias. The theoretical interband transitions wavelength are indicated by the arrows.

In Fig. 5 the observed response lies in between the GaAs and the  $\text{In}_{0.25}\text{Ga}_{0.75}\text{As}$  bandgaps, specifically within 825–940 nm. According to equation (4), the most probable transitions are from bound states with the same quantum numbers. This is clearly evidenced in the experimental data. The transition HH2-2 contributes with the peak responsivity, at approximately 840 nm. The transition HH1-1 is also noticeable at about 930 nm, and becomes stronger when high bias is applied. As intended by design, this effect occurs because the excited electrons to the conduction band ground state can tunnel more easily through the tip of the barriers, made thinner by the bending due to the applied bias. The transitions LH1-2 and HH1-2 are also possible due to the asymmetry of the quantum well and become stronger with higher bias due to the asymmetry increase caused by the bending of the potential profile. These transitions are identified in Fig. 5 at about 850 and 870 nm, respectively. As discussed above, at high bias, the extraction of the photoexcited electrons becomes easier causing

the increase in responsivity due to the other transitions from the valence bound states to the conduction band ground state, HH3-1, HH2-1, LH1-1. This effect can be observed in Fig. 5 at approximately 880, 890 and 910 nm, respectively. Additionally, the reduction of the peak response (under 4.5 V), near 840 nm, is probably because of the shifting of quasi-bound states to the continuum, which reduces the oscillator strength [2].

Another important fact that can be noticed in the NIR responsivity is that the absorption due to the light hole transitions are smaller than that due to heavy hole transitions as a consequence of degeneracy of the valence bands [1]. The fast drop of the photocurrent at about 830 nm is due to absorption of incident light by the GaAs substrate.

Finally, as observed in Fig. 5, it is possible to select the peak response of the device using bias. Voltages in between 0.5 and 4.5 V change the response shape and responsivity peak making the device adjustable.

## IV. CONCLUSIONS

Tunable narrow band NIR detection has been demonstrated using interband transitions in quantum well infrared photodetectors. A GaAs/InGaAs quantum well was fabricated. The potential profile was made asymmetric to allow interband transitions form states with different parity quantum numbers. A self-consistent calculation using the Shooting method predicted the transition wavelength peaks with great accuracy. By varying the applied bias on the device it was possible to modify the spectral response. Lower bias maximizes transitions from heavy hole first excited state to the electrons first excited state with peak around 840 nm. Higher bias maximizes transitions from heavy hole ground state to the electrons ground state with peak around 930 nm. The results demonstrate the possibility of tunable detection in the NIR band with great versatility. Furthermore, by varying the dimensions and composition of the device materials it is possible to cover virtually the entire band to fit the application requirements.

## REFERENCES

- [1] E. Rosencher and B. Vinter, *Optoelectronics*, Cambridge University Press, London, 2002, pp. 344-350.
- [2] B. F. Levine, "Quantum-well infrared photodetectors," *Journal of Applied Physics*, 74, R1, 1993.
- [3] B. R. Nag, *Physics of Quantum Wells Devices*, Kluwer Academics Press, London, 2001, pp. 86-122.
- [4] Alves, F. D. P. et al., "Three band quantum well infrared photodetector using interband and intersubband transitions," *Journal of Applied Physics*, 103, 114515, 2008.
- [5] Rogalski, A., K. Adamiec, and J. Rutkowski, *Narrow-Gap Semiconductor Photodiodes*, SPIE Press, 2000, pp. 25-89.
- [6] D. D. Coon; G. Karunasiri, "New mode of IR detection using quantum wells. *Applied Physics Letters*, "v. 45, pp. 649-652, 1984.
- [7] P. Harrison, *Quantum Wells, Wires and Dots: Theoretical and Computational Physics*, John Wiley & Sons Inc., New York, 2001, pp. 23-30.